



ISSN: 0976-3031

Available Online at <http://www.recentscientific.com>

International Journal of Recent Scientific Research
Vol. 7, Issue, 10, pp. 13645-13650, October, 2016

**International Journal of
Recent Scientific
Research**

Research Article

FABRICATION AND CHARACTERIZATION OF NEW MESOPOROUS O₃ GAS SENSOR MATERIAL; IN₂O₃

Kartharinal Punithavathy I., Nirmala E*, Johnson Jeyakumar S and Joshua Gnanamuthu S

Department of Physics, TBML College, Porayar, India

ARTICLE INFO

Article History:

Received 20th June, 2016
Received in revised form 29th August, 2016
Accepted 30th September, 2016
Published online 28th October, 2016

Key Words:

Nano indium oxide, Mesoporous, UV-Visible spectrograph, Photoluminescence, Gas sensor, Optical transparency.

ABSTRACT

In this work, the nano indium oxide (In₂O₃) powder is prepared by hydrothermal technique. The prepared powders at different mole (0.1M, 0.2M & 0.3M) were annealed at 350°, 400° and 450° C temperatures respectively. The nanopowder was optimized at 0.2 M with 400° C by XRD investigation. The XRD peak with maximum intensity at (222) plane showed the lattice; body-centered-cubic (bcc). The gas sensing functions of In₂O₃ for O₃ were tested in terms of electrical conductivity and the efficiency of present sensor in terms of response and recovery rates are very high when compared to commercial detector. The calculated particle size was in the range of 10-20 nm and the particle size was found to be almost uniform and also surface of the crystal was observed regular, which were confirmed by SEM and TEM images. The peaks of In and O in EDAX spectrum ensured the material was free from contamination. The Photoluminescence analysis proved the optical transparency of the prepared material and it is to be the main root cause of radiative centre was oxygen vacancies produced as common defects.

Copyright © Kartharinal Punithavathy I et al., 2016, this is an open-access article distributed under the terms of the Creative Commons Attribution License, which permits unrestricted use, distribution and reproduction in any medium, provided the original work is properly cited.

INTRODUCTION

Past decades, the nanometal particles have received immense attraction due to their potential applications in the field of gas sensing [Ivanovskaya et al, 2001; Gurlo et al, 1998; Doll et al, 1998]. Usually, electrochemical interaction between nano metal atoms in the surface of the nanomaterial is the basic principle of semiconducting metal oxide gas sensors. For n-type semiconductors; In₂O₃, the electronic conductivity is made by creating intrinsic oxygen vacancies in the nano crystal surface [Wagner. et al, 2009]. Usually chemical absorption made by oxygen vacancies in ambient condition creates extrinsic acceptor states that produce an assembly of electrons which repel the band electron. These condition results different electron domain regions and thereby a depletion layer is produced near the surface region. In a nano granular system, the formation of depletion layers making the potential barrier called Schottky barrier. Such a type of these barriers reduced the efficiency of electron transport system which results in the lower conductivity of the nano material. Therefore, the conductivity is controlled by the rate of surface oxygens species and vacancies. The presence of gases on the surface of the nano material with reducing properties influence the amount of oxygen, thus changes in electronic conductivity which is an easily measurable quantity for the presence and concentration of gasses under study. The nanomaterial with

large surface to volume ratio would have high accessibility for sensing applications and these facilities satisfied by high ordered mesoporous In₂O₃ structure. The evidence of such concepts was addressed by for recent research work [Tiemann. et al, 2007; Atashbara. et al, 1999; Yang. et al, 2003; Tian. et al, 2003]. The high mesoporous with low particle size nanomaterial can be acted as high sensitivity gas sensing material. In the present work, the present fabricated nanomaterial made up of 10-20 nm size particles, So far, no work on gas sensing applications has been carried out for In₂O₃ with such a low size nano particle. In this attempt, the nanomaterial is fabricated with low size and was characterized using different techniques involved in measuring the nano material and the gas sensing properties.

MATERIAL AND METHODS

Synthesis of In₂O₃

A certain amount (0.1M (1%), 0.2M (2%), 0.3M (3%)) of In (NO₃)₃ and H₂O were mixed with 1,4 -butadinol (30ml) and stirred with de-ionized water. The solution is dripped slowly in 30ml of ammonia until; a milk white precipitation appears. By dripping ammonia, the pH value was maintained as the solution was changed to alkaline, thus it was completely precipitated. The white colloidal gel was kept in a constant temperature bath at 60°C for 20 hours and it was further slowly heated until a

*Corresponding author: **Nirmala E**

Department of Physics, TBML College, Porayar, India

light brown solution. The solution was again dried at 60°C. In order to study the effect of annealing temperature on the structural, optical, and morphological properties, the prepared In₂O₃ powder was annealed at 350°, 400° and 450° C calcined for 3 hours, and pale yellow In₂O₃ nanopowder was obtained.

Analytical technique

The structural properties of In₂O₃ powder were investigated using PAN analytical X-ray diffractometer with Cu K α radiation at $\lambda = 1.5406 \text{ \AA}$. The X-ray diffraction (XRD) pattern was recorded in the range of 20 to 80 at a scanning rate of 5° min⁻¹. The Morphological studies were performed using Scanning Electron Microscopy (SEM, Hitachi S-3400N, Japan). The transmittance and absorbance spectra of the In₂O₃ powder were recorded using a UV-Vis spectrophotometer (Schimadzu 160A). Transmission Electron Microscopy (TEM) and Selected Area Electron Diffraction (SAED) were performed on a Philips CM30-ST microscope. For Energy Dispersive X-ray (EDX) analysis has been carried out by EDAX PV 9900.

The analytical ozone measurement was carried out on the detector which is working under the principle of wet chemical Brewer–Milford [Brewer .et al, 1960]. The Gas-sensing device was fabricated by drop-coating suspensions of the heat-treated powders in methanol onto silicon substrates (3 mm×3 mm) with pre-deposited platinum electrodes and heaters and pre-connected silver wires. The entire measurements were executed in a temperature-stabilized sealed chamber at 25°C with controlled humidity. The Electrical characterization was carried out by volt-amperometric technique. The electrical and gas-sensing properties of the thin film were tested using the flow-through technique.

RESULTS

Structural Characterization

The possible crystal structure of the In₂O₃ powder was presented in the Figure 1.

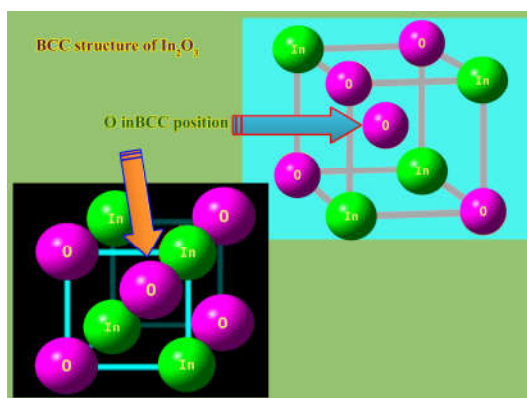


Fig 1 Crystal Structure of In₂O₃

The XRD pattern of In₂O₃ powder (0.1 M, 0.2 M and 0.3 M) substance was annealed at 350° and 400° C as shown in Figure 2. The signals from 30°, 35°, 50° and 60° were assigned to (222), (400), (440) and (622) crystal planes respectively. When compared with XRD peaks in a different mole of substances and at different annealing temperatures, it was found that, the optimized result was obtained at 0.2M with 400°C. The XRD pattern of the prepared compound confirmed that, the nano

In₂O₃ belongs to the body-centered-cubic (bcc) lattice and this result was in line with the previous work [Tanur Sinha.et al, 2014].

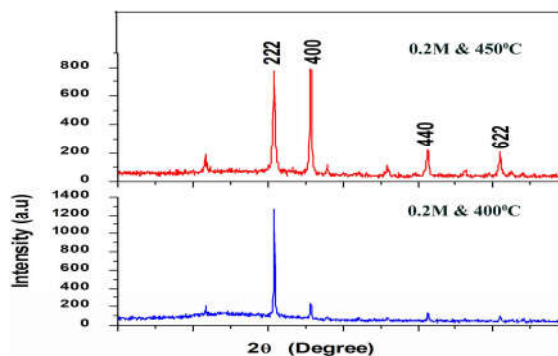


Fig 2 XRD pattern of optimized In₂O₃ (0.2 M) at 400 C & 450 C

In this case, only one peak from (222) plane was observed with maximum intensity and rest of others were found with least intensity. When comparing the peak at (222) plane with two temperatures and two molarities, it was identified that, the peak intensity was increased with increasing of annealing temperature. This view was ensured that the crystalline character of In₂O₃ is greatly enhanced at 400°C. In addition to the Bragg signals for body centered cubic (bcc) of In₂O₃ nanocrystals, supplementary unassigned crests were also found which suggested that the crystallization of other phases also occurred on the surface of the nanoparticles. This observation showed that the crystalline character of In₂O₃ is greatly enhanced which was evident from the previous work [Wang. et al, 2007]. The XRD parameters of the present compound were presented in the Table 1.

Table 1: XRD-Structural parameters of In₂O₃ powder

Molarity	Annealing temperature (°C)	Position (2θ)	(hkl)	a (Å)	FWHM	Particle size(nm)	Microstrain (ε) × 10 ⁻³	Dislocation Density(δ) × 10 ¹¹
0.1	400	30.51	222	2.92	0.34	24.96	1.4	1.5
0.2	400	30.48	222	2.92	0.42	20.46	1.7	2.3
0.3	400	35.34	222	2.53	0.39	22.11	1.6	2.0

The particle size is a very important factor since the physical and chemical property of the particle depends on the size. The present nano material was made up of heteronuclear nano atoms such as In and O. Usually the crystal was formed by In atom in O frame or O in In frame. In this case the ratio of In and O was 2:3, so that, generally O is in the corner of the cubic and In is in the body of the cubic and thus the BCC is framed up by the series bonding of In and O. According to the XRD, the average grain size of In₂O₃ was calculated by Scherrer’s equation,

$$D = k\lambda / (\beta \cos\theta), \tag{1}$$

where *D* is the grain size, β the full width at half maxima, θ is the angle of diffraction, and λ is the wavelength of X-ray (1 5406 Å). The Variation of crystallite size and microstrain (ε) different annealing temperatures were presented in the Figure 3.

Using the standard formula [Yoshi. et al, 2002], the crystal parameter values; strain (ε) and dislocation density (δ) were calculated.

The strain value ϵ can be evaluated using the following relation:

$$\epsilon = (\lambda/D\cos\theta) - (\beta/\tan\theta) \quad (2)$$

The dislocation density (δ) of powder with cubic structure has been calculated by the formula

$$\delta = 15 \epsilon/aD \quad (3)$$

From these results of In_2O_3 powder at a different annealing temperature of 350° and 400° C, it was observed that, the quality of crystal structure and the optical properties of In_2O_3 nanopowder were greatly improved with respect to temperature. The variation of a crystallite size at different annealing temperature was given in the Table 1. The calculated crystal size at 0.2M with 400°C was found to be 20.46 nm which was so reduced in size and is capable of having large applications. In this case, the annealing time and temperature are very important parameters since they enhance the physical and optical quality of the powder. Similarly, when the annealing temperature was used beyond 400°C , the powders were not with good amalgamation. So it is better to maintain the annealing temperature at 400°C for the present case. The Scherrer's equation suggests that the crystal domain sizes are in the region of 20.46 nm, and it was less than the repetition distance of the mesopores. This view showed the presence of regularly arranged mesopores which not distort the nano size crystallinity of In_2O_3 .

Morphological studies

The morphological view of the In_2O_3 powder was observed in SEM images which were depicted in the Figure 3.

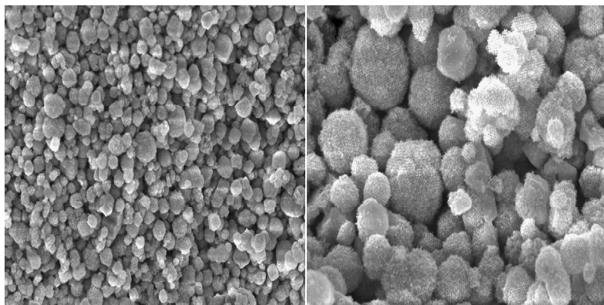


Fig 3 SEM images of small (left) and large particles (right)

Scanning electron microscopy technique (SEM) was mainly used for morphological characterization at the nanometer to micrometer scale [Erol. *et al*, 2009]. Here the SEM images show uniformly distributed indium oxide nanoparticles in the crystal lattice which indicates that the stabilization of nanoparticles is in suitable position of the cubic system and the size distribution of the mesoporous particles (secondary particles) was analyzed by SEM. From the SEM image, it was also found that the indium nanoparticles were spherical in shape and the mesostructure of the particles is clearly visible. Also, it can be seen that there is only a very small amount of non-structured In_2O_3 .

From the SEM images, it was observed that, when the annealing temperature increases from 350° C to 400° C, small particles on the surface of the film can be seen clearly. Further if the temperature was increased from 400° to 450° C, it can be viewed that, the agglomeration of the In_2O_3 particles present in

the surface of the powder. Such agglomeration process may be attributed due to the lower melting point of In_2O_3 .

TEM analysis

The clear structural morphology and accurate particle size of the indium oxide nanoparticles can be determined by TEM and SAED images. A Transmission Electron Microscope (TEM) utilizes energetic electrons to provide morphologic, compositional and crystallographic information of samples. At a maximum potential magnification of 2 nanometers, TEMs are the most powerful microscopes. TEMs produce high-resolution, two-dimensional images, allowing for a wide range of electronic, biological, pharmaceutical and industrial applications.

The analytical TEM and SAED view were presented in the Figures 4 and 5 respectively. The magnified image of nanocrystal; In_2O_3 powder with the bright field image, selected area diffraction pattern, and lattice fringe were identified in the pictures. The Particle agglomeration was clearly observed and the particle size was determined as 10-45 nm, the range which was consistent with the XRD results (Figure 4).

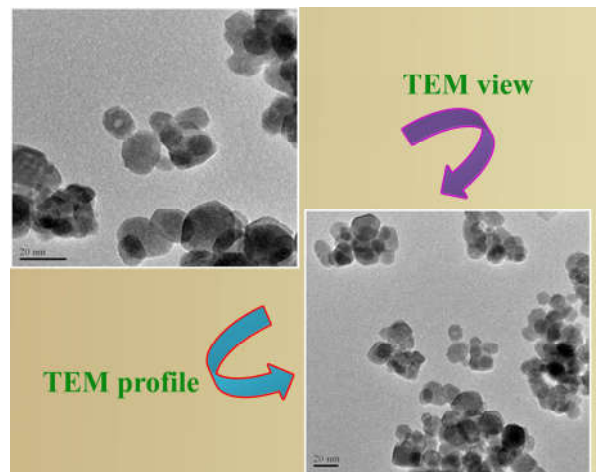


Fig 4 TEM images of Indium Oxide

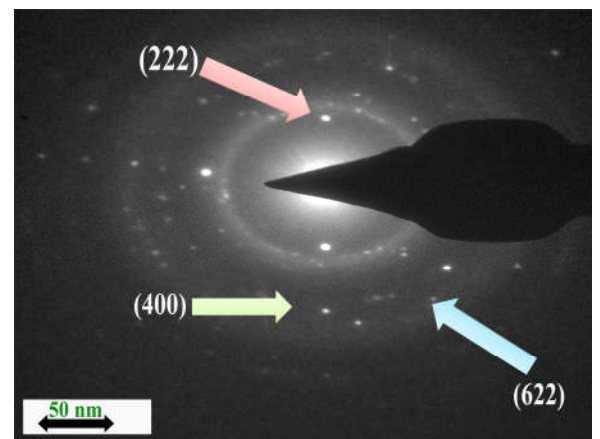


Fig 5 SAED pattern

The selected area diffraction pattern (SAED) showed the major peaks correspond to In_2O_3 powder and were consistent with the results obtained in XRD analysis. The pattern of SAED in the Figure 5 contained dots and diffused concentric diffracted rings which obviously showed the well crystallization of In_2O_3 powder. The spots could be indexed corresponding to the reflections from the diffraction planes of (222), (400), (440)

and (622) respectively. The pattern of the SAED consists of distinct spots, indicating large single-crystalline domains extending over several repetition distances of the mesopores and also ensured that the crystal formation of In₂O₃ powder belongs to BCC lattice.

Sensor device characterization

The Electrical characterization has been carried out by two steps. In the first attempt, the conductive property of the films was studied under atmospheric environment and in the second step, the sensing capability of the layers toward O₃ was analyzed. The optimized temperature for good sensor response was determined and was found to be 200°C. The isothermal characterization as a function of ozone concentration in the range 0-300 ppb was displayed in the Figure 6.

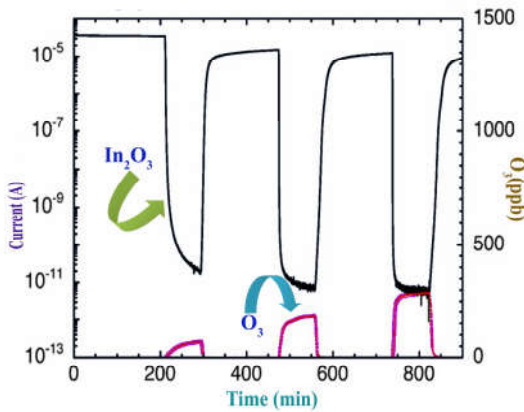
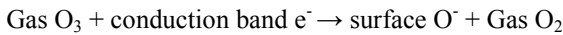


Fig 6 Sensor Response for indium oxide powder

Usually, the conductance of the film decreases due to the interaction of ozone on the oxide surface which increases the oxide resistance. The mechanism involved in the reaction can be distributed as



During the measurement process, the In₂O₃ sensor response is very high and the conductance changes fivefold of magnitude in presence of ozone less than 200 ppb. In this case, the sensor response is reproducible and stable at the operating temperature, in which, the baseline was not completely vanished after the ozone termination. Beyond 300° C, though the response is found to be low which indeed keeps at an elevated level, but the response and the revival turned into quicker and absolute. The kinetic response of the In₂O₃ to 60 ppb of ozone is presented in the Figure 7. Furthermore, the efficiency of the present sensor in terms of response and recovery rates are enough very high when compared to the commercial detector, the response is showed as dotted line in the respective Figure. The indium oxide based sensor response has taken up 7 min for 5%–90% whereas the commercial sensor has taken 45 min for the step 10–85% of 180 ppb ozone concentration.

As per the previous report [Mauro Epifani. et al, 2008], the mechanism related to sensor response regarding ozone is due to the basic principle of standardized variation of resistance of an n type semiconductor transducer.

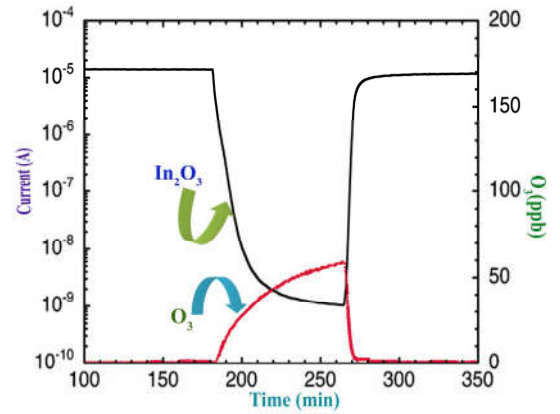


Fig 7 Response of the In₂O₃ to 60 ppb of ozone

Figure 7 showed the response of indium oxide layers as a function of the concentration of ozone introduced in the test chamber at working temperature 200°C. In metal-oxide-semiconductor sensing films, the sensor response depends upon the gas concentration [Madou . et al, 1998; Gurlo . et al, 1997]. In this case, as the operating temperature is 200°C; the response of the film is significantly good as compared to metal-oxide semiconductor films in the earlier works [Baratto . et al, 2006; Sucheai . et al, 2006]. From this observation, it was inferred that, since the gas sensing application of the present nanomaterial (In₂O₃) was better than commercial sensor materials, it will fine to fabricate the sensing device using nano indium oxide compound.

Optical studies

UV-Visible absorption measurements in the wavelength range of 460 nm [Wang .et al, 2000; Pal. Et al, 2007; Huang . et al, 2004] were used in characterizing the indium oxide nanoparticles. This characteristic peak is due to the electronic transition of In-O. UV-vis spectroscopy was ascertained to check the formation and stability of In-O nanoparticles.

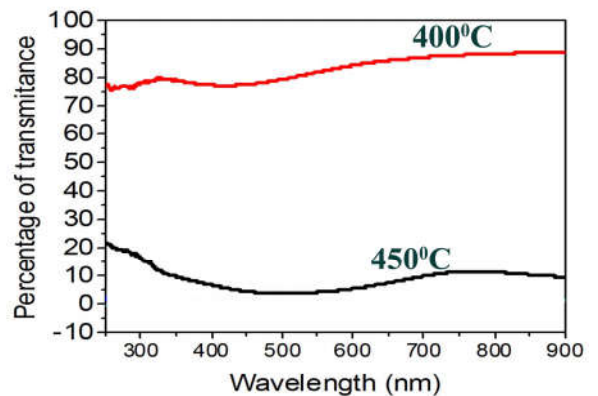


Fig 8 UV-Visible absorbance spectrum of In₂O₃ powder

Figure 8 shows the UV-Visible absorbance spectrum of In₂O₃ powder annealed at above said temperatures. From the figure, it was observed that the signal at 550 nm with high absorption, i.e. 72%. Further, it was found that, the optical absorption was occurred in the 1.5 –1.6 eV (photon-energy range). This result of the present study well agreed with the previous work [Chawla. et al, 2008; Swanepoel. et al, 1983]. From this observation, it was concluded that, the electronic absorption found exactly at a green wavelength in visible region. So the

material is able to have the O₃ gas sensing property well. In this case, the peak intensity is more than 70% which is a reasonable one. The amplification of the peak intensity reflected the rate of concentration of O vacancies in the material [Zhang. *et al*, 2006]. Accordingly, the present material; indium oxide nanoparticles has sufficient mesoporous structure. In this analysis, the peak with maximum intensity was observed at the annealed temperature about 400°C than rest of samples.

For the direct or indirect optical transitions in the band gap, the optical absorption coefficient can be analyzed by using the following equations [Chawla. *et al*, 2008]:

$$\alpha h\nu = A(h\nu - E_g)^m \text{ for } h\nu > E_g, \quad (4)$$

$$\alpha h\nu = 0 \text{ for } h\nu < E_g, \quad (5)$$

where α is the absorption coefficient, A is a constant depending on the band, $h\nu$ is the photon energy, E_g is the optical bandgap, $m = 2$ indicates an allowed indirect transition and $m = 0.5$ indicates an allowed direct transition. The optical band gap was estimated by extrapolating the straight line of $(\alpha h\nu)^{1/2}$ versus the photon energy curve as shown in Figure 9.

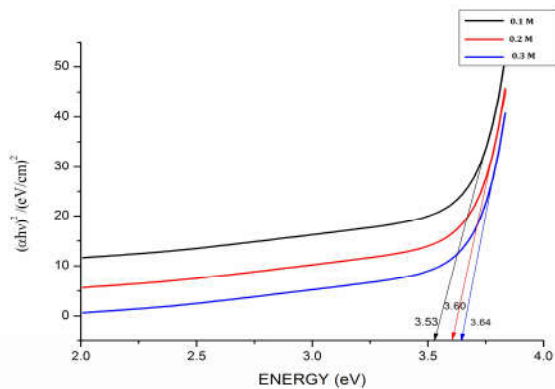


Fig 9 Tauc plot for (0.1,0.2 & 0.3 M) indium oxide powder

The intercept of the tangent to the plot provided a good approximation of the band gap energy value of In₂O₃ powders. The extrapolations of these linear sections yield band gaps; $E_{400^\circ\text{C}} = 3.50$ eV and $E_{450^\circ\text{C}} = 3.64$ eV. From the calculations, it was found that, the band gap of the In₂O₃ powder was gradually increased from 3.53 and 3.64 eV due to increasing of annealing temperature.

Photoluminescence studies

The photoluminescence analysis used to analyze the alloys in homogeneities and variations in impurity concentration which arise owing to the preparation of nanopowder with different heteronuclear atoms. It is observed that the photoemission wavelength is independent of the particle size while the intensity increases sharply with a decrease of particle size. This visible luminescence of In₂O₃ is due to excitation of electrons from occupied bands into states above the Fermi level. The PL spectra were recorded using an excitation wavelength of 373 nm and shown in Figure 10.

Among these bands, the band at 424 nm was attributed to near ultraviolet emission which was due to the presence of oxygen vacancies and the observation was agreed well with the earlier

reports [Baloukas. *et al*, 2011; Park . *et al*,2011; Niederberger. *et al*,2002].

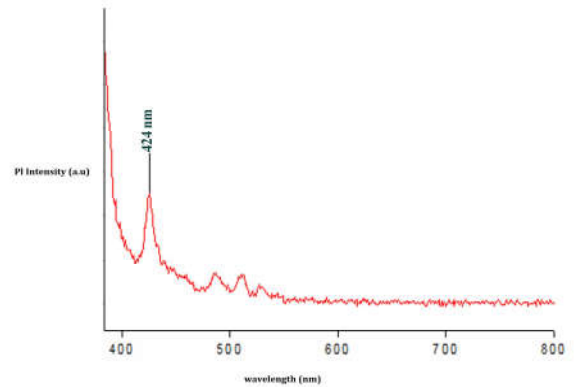


Fig 10 Photoluminescence Studies

The refractive index (n) of the powder was determined from the optical transmittance using the following relation [Luo. *et al*, 2007]:

$$R = \frac{(n - 1)^2 + K^2}{(n + 1)^2 + K^2} \quad (6)$$

Where R is the reflectance values of the In₂O₃ powder

$$\text{Extinction coefficient } K = \frac{\alpha\lambda}{4\pi}$$

where n and K are the refractive index and extinction coefficient of powders respectively.

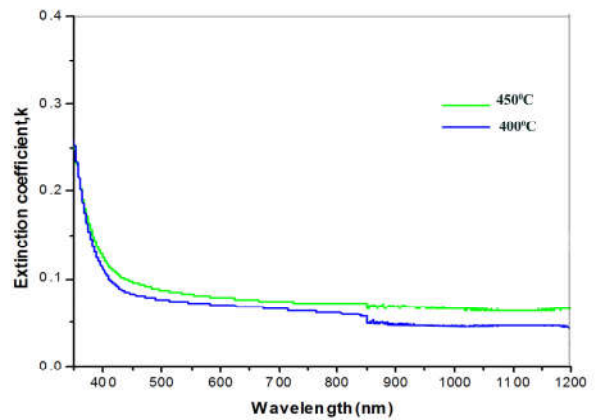


Fig 11 Extinction Coefficient

Figure 11 shows the wavelength dependence of refractive index of In₂O₃ powder formed without different oxygen partial pressure. For all powders, the refractive index values are found decreasing with the increase of wavelength. From the observation, it was important to note that, the refractive index increases from 2.2 to 2.3 with the increase of annealing temperature.

CONCLUSION

The nano indium oxide (In₂O₃) powder was prepared on simple hydrothermal technique and was annealed at different temperatures. The XRD investigation has been carried out and their results ensured that the material with a high degree of crystallinity and mesoporous structure. The annealing process has certainly improved the crystallization of the powder,

particularly at 400°C. The SEM and TEM results confirmed the particle size in the range of 10–45 nm. The peaks corresponding to the In and O in EDAX spectrum ensure the powder is purely made up of nano In₂O₃ and it was free from the contamination. The mesoporous In₂O₃ gained by nano fusing exposed exceptional structural properties for gas sensors. The structure of the material is readily accessible to ozone gas molecules. The morphology of the sensor can be varied significantly and even ordered mesoporous materials can be easily fabricated using the technique used in this work. The UV-Visible study was explicated the optical ability of the nano In₂O₃. The Photoluminescence analysis revealed that, the optical transparency of the powder and it was found that, the powder was able to convert the green light to electronic energy.

References

- Ivanovskaya M., Gurlo A., Bogdanov P., (2001) Sens. Actuators, B, Chem. 77, 264.
- Gurlo A., Bârsan N., Ivanovskaya M., Weimar U., Göpel W., (1998) Sens. Actuators, B, Chem. 47, 92.
- Doll Th., Fuchs A., Eisele I., Faglia G., Groppelli S., Sberveglieri G., (1998) Sens. Actuators, B, Chem. 49, 63.
- Wagner T., Sauerwald T., Kohl C.D., Waitz T., Weidmann C., Tiemann M., (2009) Thin Solid Films 517: 6170–6175.
- Tiemann M., (2007) Chem. Eur. J. 13: 8376
- Atashbara M.Z, Gongb B., Sunc H.T, Wlodarskia W., Lamb R., (1999) Thin Solid Films 354: 222–226.
- Yang H., Shi Q., Tian B., Lu Q., Gao F., Xie S., Fan J., Yu C., Tu, B. Zhao D., (2003) *J. Am. Chem. Soc.* 125: 4724.
- Tian B., Liu X., Yang H., Xie S., Yu C., Tu B., Zhao D., (2003) *Adv. Mater.* 15 :1370.
- Brewer A.W., Milford J.R. Proceedings of the Royal Society (1960) A, 256, 470.
- Tanur Sinha, M. Ahmaruzzaman, Archita Bhattacharjee, Mohammad Asif V.K. Gupta, (2014) *Journal of Molecular Liquids* 01: 13–22.
- Wang J, Sallet V, Jomard F, Rego A M, Elamurugu E, Martins R and Fortunato E 2007 *Thin Solid Films* 515: 8785.
- Hoshi Y., Kiyomura T., (2002) *Thin Solid Films* 411: 36.
- Erol M., Han Y., Stanley S.K., Stafford C.M., Du H., Sukhishvili S., (2009) *J. Am. Chem. Soc.* 131, 7480.
- Mauro Epifani and Elisabetta Comini (2008) *Sensors and Actuators B* 130: 483–487.
- Madou M.J., Morrison S.R., (1988) *Chemical Sensing with Solid State Devices*, Academic Press Inc., New York, pp. 67–104.
- Gurlo A. and Ivanovskaya M., (1997) *Sensors and Actuators B* 44: 327–333.
- Baratto C., Ferroni M., Faglia G., Sberveglieri G., (2006) *Sensors and Actuators B* 118: 221–225.
- Suchea M., Katsarakis N., Christoulakis S., Nikolopoulou S., Kiriakidis G., (2006) *Sensors and Actuators B* 118: 135–141.
- Wang X., Bunkers G.J., (2000) *Res. Commun.* 279 669.
- Pal S., Tak Y.K., Song J.M., (2007) *Appl. Environ. Microbiol.* 73: 1712.
- Huang H., Yang X., (2004) *Carbo hydr. Res.* 339: 2627.
- Chawla A. K., Singhal S., Gupta H. O., and Chandra R., (2008) *Thin Solid Films*, 517, 3, 1042–1046.
- Swanepoel R., (1983) *Journal of Physics E*, 16, 12, 1214.
- Zhang W.Z., Qiao X.L., Chem J.G., (2006) *Chem. Phys.* 300: 495–500.
- Baloukas B., Lamarre J. M., and Martinu L., (2011) *Solar Energy Materials and Solar Cells*, vol. 95, no. 3, pp. 807–815.
- Park S., Kim H., Jin C., and Lee C., (2011) *Nanoscale Research Letters*, vol. 6, p. 451.
- Niederberger M., Bartl M. H., and Stucky G. D., (2002) *Journal of the American Chemical Society*, vol. 124, no. 46, pp. 13642–13643.
- Luo J. Y., Zhao F. L., Gong L. (2007) *Applied Physics Letters*, vol. 91, no. 9, 3.

How to cite this article:

Kartharinal Punithavathy I et al., Fabrication and Characterization of New Mesoporous O₃ Gas Sensor Material; IN₂O₃. *Int J Recent Sci Res.* 7(10), pp. 13645–13650.